

- $\delta(\text{CF}_2\text{Cl}_2) = 0$ , external):  $\delta = -136.9$  (d, 2F,  $J(\text{F},\text{F}) = 8.4$  Hz;  $\text{F}^{\text{meta}}$ ),  $-167.7$  (tr, 1F,  $J(\text{F},\text{F}) = 20.7$  Hz;  $\text{F}^{\text{para}}$ ),  $-171.5$  (tr, 2F,  $J(\text{F},\text{F}) = 16.8$  Hz;  $\text{F}^{\text{ortho}}$ );  $^{13}\text{C}\{^1\text{H}\}$  NMR (100.63 MHz,  $[\text{D}_6]\text{benzene}$ , 300 K,  $\delta(\text{C}_6\text{D}_6) = 128.0$ ):  $\delta = 185.8$  (s;  $\text{C}^{\alpha}$ ), 149.1 (d,  $^1J(\text{C},\text{F}) = 241.5$  Hz;  $\text{C}^{\text{meta}} [\text{B}(\text{C}_6\text{F}_5)_4]$ ), 143.0 (s;  $\text{C}^{\text{para}}$ ), 141.6 (s;  $\text{C}^{\text{ortho}}$ ), 139.2 (d,  $^1J(\text{C},\text{F}) = 251.6$  Hz;  $\text{C}^{\text{para}} [\text{B}(\text{C}_6\text{F}_5)_4]$ ), 137.0 (d,  $^1J(\text{C},\text{F}) = 251.6$  Hz;  $\text{C}^{\text{ortho}} [\text{B}(\text{C}_6\text{F}_5)_4]$ ), 130.9 (s;  $\text{C}^{\text{meta}}$ ), 125.2 (br;  $\text{C}^{\text{ipso}} [\text{B}(\text{C}_6\text{F}_5)_4]$ ), 113.7 (s;  $\text{C}^{\beta}$ ), 84.1 (s;  $\text{C}^{\beta}$ ), 16.3 (s;  $\text{C}^2$ ), 15.0 (s;  $\text{C}^{1/3}$ ),  $-0.7$  (s;  $\text{CH}_3$ );  $^{29}\text{Si}\{^1\text{H}\}$  NMR (79.50 MHz,  $[\text{D}_6]\text{benzene}$ , 300 K,  $\delta((\text{H}_3\text{C})_2\text{SiHCl}) = 11.7$ , external):  $\delta = 22.8$ .
- [16] a) H.-U. Siehl in *Dicoordinated Carbocations* (Eds.: P. J. Stang, Z. Rappoport), Wiley, Chichester, 1997, chapter 5, pp. 189–263; b) cf. ref. [9c, d].
- [17] a) M. Kira, T. Hino, H. Sakurai, *Chem. Lett.* **1993**, 153; b) S. R. Bahr, P. Boudjouk, *J. Am. Chem. Soc.* **1993**, 115, 4514; c) Z. Xie, D. J. Liston, T. Jelinek, V. Mitro, R. Bau, C. A. Reed, *J. Chem. Soc. Chem. Commun.* **1993**, 384; d) J. B. Lambert, S. Zhang, S. M. Ciro, *Organometallics* **1994**, 13, 2430.
- [18] Spectroscopic data of **4a**:  $[\text{B}(\text{C}_6\text{F}_5)_4]$  (For spectroscopic data of the anion, see **4b**).  $^1\text{H}$  NMR (400.14 MHz,  $[\text{D}_6]\text{benzene}$ , 300 K,  $\delta(\text{C}_6\text{D}_6) = 7.20$ ):  $\delta = 1.42$  (s, 3H;  $\text{C}^{\alpha}\text{-CH}_3$ ), 1.26 (m, 2H;  $\text{H}^2$ ), 0.4–0.3 (m, 4H;  $\text{H}^{1/3}$ ),  $-0.06$  (s, 12H;  $\text{CH}_3$ );  $^{13}\text{C}$  NMR (100.63 MHz,  $[\text{D}_6]\text{benzene}$ , 300 K,  $\delta(\text{C}_6\text{D}_6) = 128.0$ ):  $\delta = 184.8$  (q,  $^2J(\text{C},\text{H}) = 9$  Hz;  $\text{C}^{\alpha}$ ), 77.7 (s;  $\text{C}^{\beta}$ ), 15.9 (t,  $^1J(\text{C},\text{H}) = 131$  Hz;  $\text{C}^2$ ), 15.0 (t,  $^1J(\text{C},\text{H}) = 126$  Hz;  $\text{C}^{1/3}$ ), 9.3 (q,  $^1J(\text{C},\text{H}) = 136$  Hz;  $\text{C}^{\beta}$ ),  $-0.8$  (q,  $^1J(\text{C},\text{H}) = 121$  Hz;  $\text{Si}(\text{CH}_3)_2$ );  $^{29}\text{Si}\{^1\text{H}\}$  NMR (79.50 MHz,  $[\text{D}_6]\text{benzene}$ , 300 K,  $\delta((\text{H}_3\text{C})_2\text{SiHCl}) = 11.7$ , external):  $\delta = 9$ .
- [19] Y. Apeloig, T. Müller in *Dicoordinated Carbocations* (Eds.: P. J. Stang, Z. Rappoport), Wiley, Chichester, 1997, chapter 2, p. 9.
- [20] NBO analysis was done at B3LYP/6-31G(d)/B3LYP/6-31G(d). a) NBO 4.0: E. D. Glendening, J. K. Badenhoop, A. E. Reed, J. E. Carpenter, F. Weinhold, Theoretical Chemistry Institute, University of Wisconsin, Madison, WI, 1996; b) A. E. Reed, L. A. Curtiss, F. Weinhold, *Chem. Rev.* **1988**, 88, 899.
- [21] For calculating Equation (1b), the energy of the less stable isomer **Z-8(H)** was used. The conformation of the phenyl group relative to the C=C bond is in **Z-8(H)** (dihedral angle  $\text{C}^{\text{ortho}}\text{-C}^{\text{ipso}}\text{-C-C} \theta = 33.7^\circ$ ) very similar to that in **4b(H)** ( $\theta = 31.0^\circ$ ), while in **E-8(H)** phenyl ring and C=C bond are coplanar ( $\theta = 0.0^\circ$ ). Using the energy of **E-8(H)** in Equation (1b) would include the more favorable conjugation between the C=C bond and the phenyl substituent. Thus, the comparison between **4b** and **8** would be not balanced.

## [(Cp\*RuCl)<sub>2</sub>(μ-Cl)<sub>2</sub>]: Bond-Stretch or Spin-State Isomerism?\*

John E. McGrady\*

The phenomenon of bond-stretch isomerism,<sup>[1]</sup> the ability of a single molecule to exist in two distinct forms differing only in the length of one or more bonds, has been the source of intense debate ever since the first example, *cis-mer*-[Mo(O)Cl<sub>2</sub>(PMe<sub>2</sub>Ph)<sub>3</sub>], was reported by Chatt and co-workers.<sup>[2]</sup> Related examples such as [W(O)Cl<sub>2</sub>(Me<sub>3</sub>tacn)]<sup>+</sup><sup>[3]</sup> (Me<sub>3</sub>tacn = *N,N',N''*-trimethyl-1,4,7-triazacyclononane) and [Nb(O)Cl<sub>3</sub>(PMe<sub>3</sub>)]<sup>[4]</sup> subsequently emerged, and appeared to

establish bond-stretch isomerism as a general feature of the chemistry of metal–ligand multiple bonds. This new form of isomerism naturally aroused much interest among theoretical chemists, notably Hoffmann and co-workers, who used extended Hückel theory to study strained cyclic hydrocarbon species,<sup>[1]</sup> and, much later, the metal–oxo species noted above.<sup>[5]</sup> As a result of these calculations, they postulated that a redistribution of electrons within the  $\pi$  framework of the molecule, involving either a crossing of occupied and unoccupied orbitals or a second-order Jahn–Teller effect, could account for the isomerism in [W(O)Cl<sub>2</sub>(Me<sub>3</sub>tacn)]<sup>+</sup> and *cis-mer*-[Mo(O)Cl<sub>2</sub>(PMe<sub>2</sub>Ph)<sub>3</sub>], respectively. In 1991, however, Hall and Song used more sophisticated ab initio methods to reinvestigate these claims, and reported that they were unable to locate a double minimum on the potential energy surface in either case.<sup>[6]</sup> At around the same time, a reexamination of the structure of *cis-mer*-[Mo(O)Cl<sub>2</sub>(PMe<sub>2</sub>Ph)<sub>3</sub>] showed that the apparently different Mo=O bond lengths were in fact an artifact of compositional disorder, caused by traces of *mer*-[MoCl<sub>3</sub>(PMe<sub>2</sub>Ph)<sub>3</sub>].<sup>[7]</sup> This report, in conjunction with the available theoretical data, prompted Parkin to observe in his 1993 review that there was “presently no definitive evidence of bond-stretch isomerism”.<sup>[8]</sup>

Three years previously, Kölle and co-workers<sup>[9]</sup> had reported that two isomers were present in the unit cell of [(Cp\*RuCl)<sub>2</sub>(μ-Cl)<sub>2</sub>] (**1**) (Cp\* = C<sub>5</sub>Me<sub>5</sub>; Figure 1) with very different Ru–Ru separations, 2.930(1) Å (**1a**) and 3.752(1) Å (**1b**). This system has not, however, been widely accepted as

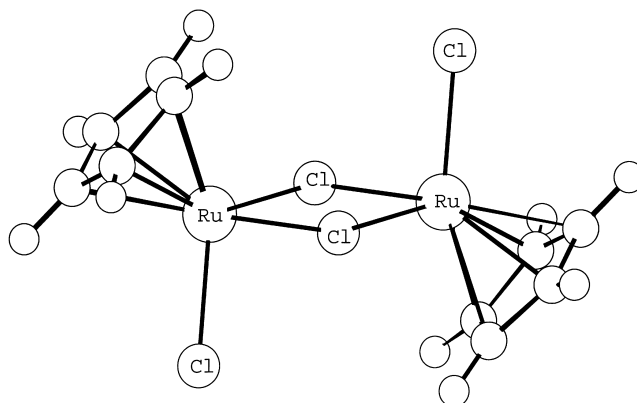


Figure 1. Molecular structure of [(Cp\*RuCl)<sub>2</sub>(μ-Cl)<sub>2</sub>] (**1**).

an example of bond-stretch isomerism because the nature of the coupling between the metal ions differs in the two isomers: antiferromagnetic in **1a**, ferromagnetic in **1b**. Hoffmann and Parkin have gone to some lengths<sup>[10]</sup> to distinguish “bond-stretch” isomerism, where both isomers lie on the same potential energy surface, from “spin-state” isomerism, where a change in multiplicity occurs.<sup>[11]</sup> Within the limits of Hoffmann’s definition, the Kölle complex is therefore properly classified as an example of “spin-state” isomerism. Herein broken-symmetry density functional theory is used to establish the fundamental electronic reasons for the co-existence of two isomers in **1**. The validity of the distinction between “bond-stretch” and “spin-state” isomerism is then reexamined in the context of dimetallic clusters.

[\*] Dr. J. E. McGrady  
The Department of Chemistry  
The University of York  
Heslington, York, YO10 5DD (U.K.)  
Fax: (+44) 1904-432516  
E-mail: jem15@york.ac.uk

[\*\*] This work was supported by the EPSRC. Cp\* = C<sub>5</sub>Me<sub>5</sub>.

Optimization of the structure of the broken-symmetry state of  $[(\text{CpRuCl})_2(\mu\text{-Cl})_2]$  ( $\text{Cp} = \text{C}_5\text{H}_5$ ) does indeed reveal two minima, denoted  $\text{S}_1$  and  $\text{S}_2$ , depending on the starting geometry. The calculated Ru–Ru separations of 2.881 Å and 3.753 Å (Table 1) for  $\text{S}_1$  and  $\text{S}_2$ , respectively, are remarkably similar to those in **1a** and **1b**, as are the other bond lengths and angles. Whilst both  $\text{S}_1$  and  $\text{S}_2$  correspond to spin singlet

Table 1. Optimized structural parameters, spin densities, and relative energies of  $\text{S}_1$ – $\text{S}_3$  and  $\text{T}_1$ . Structural parameters of **1a** and **1b** are shown for comparison.

	Ru–Ru [Å]	Ru–Cl <sup>[a]</sup> [Å]	Ru–Cl <sub>br</sub> <sup>[a]</sup> [Å]	Ru–C [Å]	Cl <sub>i</sub> –Ru–Ru <sup>[a]</sup> [°]	Spin density	$E_{\text{rel}}$ [kJ mol <sup>−1</sup> ]
calculated values							
$\text{S}_1$	2.881	2.429	2.422	2.259	88.2	0.0	0.0
$\text{S}_2$	3.753	2.370	2.480	2.263	93.4	± 0.71	+ 4.0
$\text{S}_3$	3.658	2.409	2.463	2.252	89.8	± 0.61	+ 9.0
$\text{T}_1$	3.782	2.377	2.464	2.259	94.7	+ 0.68	+ 1.0
crystallographic values							
<b>1a</b>	2.930(1)	2.418(2)	2.366(1)	2.191	89.7		
<b>1b</b>	3.752(1)	2.365(2)	2.445(1)	2.173	95.8		

[a] t = terminal Cl atom, br = bridging Cl atom.

configurations, the distribution of the ten valence electrons within the twelve spin orbitals of the  $t_{2g}$  manifold differs:  $(a')^6(a'')^4$  in  $\text{S}_1$ , and  $(a')^8(a'')^2$  in  $\text{S}_2$ . In  $\text{S}_1$ , a net spin density of zero at each metal center indicates that all orbitals are completely delocalized. The Ru–Ru  $\sigma^*$  character in the LUMO ( $4a'$ , Figure 2a) confirms that a single  $\sigma$  bond is present, as postulated previously by Burdett et al.<sup>[9b]</sup> In  $\text{S}_2$ , in contrast, the spin- $\alpha$  and spin- $\beta$  orbitals are localized on opposite sides of the molecule (Figure 2b), as a result of which, nonzero spin densities ( $\pm 0.71$  electrons) emerge at each ruthenium center. Full potential energy curves for the two configurations,  $(a')^6(a'')^4$  and  $(a')^8(a'')^2$ , are shown in Figure 3 (full and dashed lines, respectively). For the former,

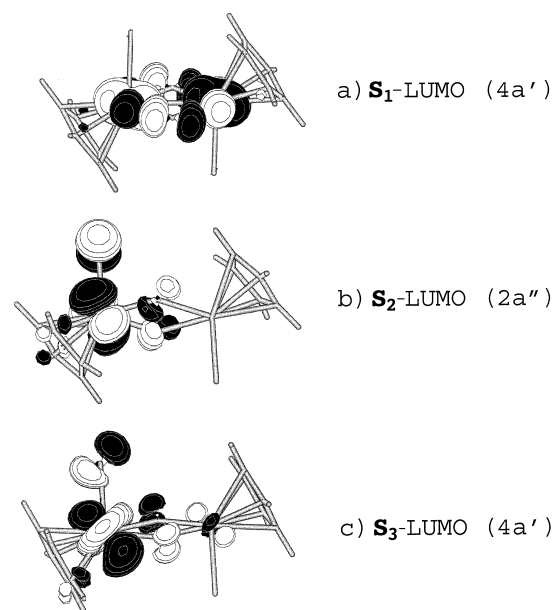


Figure 2. Lowest unoccupied spin orbitals of  $\text{S}_1$ – $\text{S}_3$ . The orbitals shown have  $\alpha$  spin; the corresponding spin- $\beta$  orbitals are mirror images of those shown.

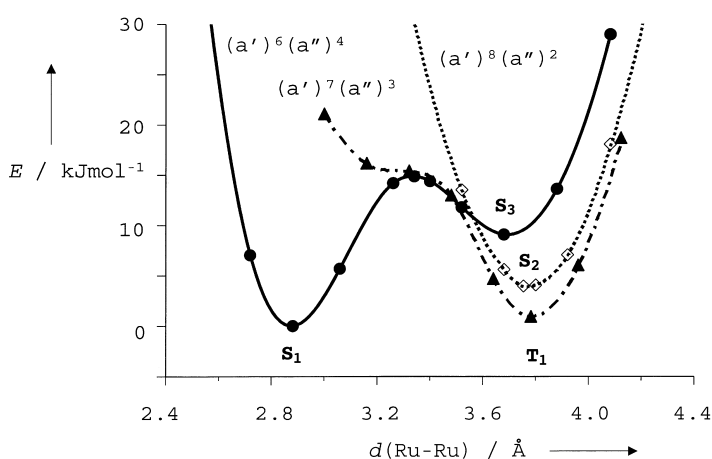


Figure 3. Potential energy curves for singlet and triplet configurations of  $[(\text{CpRuCl})_2(\mu\text{-Cl})_2]$ .

a local minimum ( $\text{S}_3$ ) is found at Ru–Ru = 3.658 Å, in addition to the one at 2.881 Å ( $\text{S}_1$ ). The double minimum arises because both Ru–Ru  $\sigma$  and  $\pi$  orbitals transform as  $a'$  in  $C_s$  symmetry, and at  $\text{S}_3$ ,  $\pi$  character, rather than  $\sigma$  character, dominates in the LUMO (Figure 2c). Although configuration interaction cannot be explicitly accommodated within the confines of density functional theory, its influence on the potential energy curves in Figure 3 can be deduced readily. Both configurations give rise to states of  $^1A'$  symmetry and so configuration interaction will mix the two, most strongly in the region where the curves cross. This mixing causes the singlet ground state to pass smoothly from the covalently bonded limit ( $\text{S}_1$ ) to the weakly antiferromagnetically coupled state ( $\text{S}_2$ ).

The location of two widely separated minima on the potential energy surface clearly indicates the existence of two distinct electronic mechanisms for conferring stability on the molecule. At short separations the primary stabilizing force is the  $\sigma$  bond between the metal atoms. At longer separations the loss of this  $\sigma$ -bond is offset by an increase in the exchange energy associated with the nonzero spin density on each individual metal center.<sup>[12a, 13]</sup> Where the covalent bonding and exchange stabilization are of similar magnitude, as they are in this case, two distinct minima can emerge on the potential energy surface. In the absence of ligands bridging the two metal centers, the weakly coupled limit simply corresponds to the dissociation limit of the bond. Thus a bridged bimetallic core is the minimum structural motif required for the occurrence of two distinct minima.

Whilst the calculated structural parameters of  $\text{S}_2$  are very similar to those of isomer **1b**, the singlet spin state is inconsistent with the experimentally observed ferromagnetism.<sup>[9]</sup> At long Ru–Ru separations, however, three triplet configurations are also present in the valence region. These configurations correspond to single occupation of a) two orbitals of  $a'$  symmetry, b) two orbitals of  $a''$  symmetry, and c) one orbital of each symmetry. Of these, only the third configuration  $(a')^7(a'')^3$ , in which the two singly occupied orbitals are orthogonal, has a ground state ( $\text{T}_1$ ) that is more stable than  $\text{S}_2$ . The Ru–Ru separations of  $\text{S}_2$  and  $\text{T}_1$  are very similar, and so, based on both structural and energetic

evidence the prime candidates for the ground states of the isomers **1a** and **1b** appear to be **S<sub>1</sub>** and **T<sub>1</sub>**, respectively. The relative energies of **S<sub>1</sub>** and **T<sub>1</sub>** are consistent with the greater observed stability of **1a**, although the calculated separation of only 1 kJ mol<sup>-1</sup> is substantially lower than the experimental value of 15 kJ mol<sup>-1</sup>. It has been noted previously, however, that the gradient-corrected density functionals used in this work tend to underestimate the strength of metal–metal bonds.<sup>[12b]</sup> If the calculations are repeated without gradient corrections the general features of the curves remain unchanged but the **S<sub>1</sub>**–**T<sub>1</sub>** energy separation rises to 50 kJ mol<sup>-1</sup>, substantially higher than the experimental estimate. The purpose of this paper is not to assess the merits of different functionals and this comparison is provided simply to illustrate that the calculation of relatively small energy differences remains a considerable challenge to computational chemistry. In the present context, the critical point to emphasize is that density functional theory predicts the presence of two minima on the potential energy surface with an energetic separation that is consistent with the coexistence of two isomers in a single crystal. The calculated barrier that separates the two minima (15 kJ mol<sup>-1</sup>) is also consistent with experiment, being low enough to allow rapid equilibration in solution, but high enough to prevent interconversion in the solid state.

Having established the physical basis for the coexistence of two distinct isomers we can now address the question raised in the title—should the Kölle complex be classified as an example of “bond-stretch” or “spin-state” isomerism? In the strict Hoffmann definition the answer is clearly the latter because a change of spin state does occur. However, the nature of the spin-state transition in dimetallic species is distinctly different from that in monomeric spin–crossover complexes. In the latter, the low-spin/high-spin transition is intrinsically linked to the change in structure, because metal–ligand antibonding orbitals must be populated in the high-spin state. In contrast, in dimetallic systems the spin-state transition involves only a reorientation of spins on the metal centers and is associated with very minor structural changes (compare the structures of **S<sub>2</sub>** and **T<sub>1</sub>**). Moreover, the underlying stabilizing mechanism, the exchange energy, is the same in both **S<sub>2</sub>** and **T<sub>1</sub>**. There is therefore no *causal* link between the change in structure and the change in spin state. The isomerism observed in complex **1** is, in fact, best described as an equilibrium between a covalently bonded species and a diradical. When viewed in this context the system is very similar to the strained cyclic hydrocarbon species that formed the basis of Hoffmann’s original work on bond-stretch isomerism.<sup>[1]</sup> In summary, despite the change in spin state associated with the isomerism in **1** this system fulfills all the criteria required of “bond-stretch” isomerism, and should be recognized as a genuine example thereof.

### Computational Methods

All calculations were performed by using the Amsterdam Density Functional (ADF99) program.<sup>[14]</sup> Double- $\zeta$  + polarization and triple- $\zeta$  basis sets were used to describe the main group and ruthenium atoms, respectively. The local density approximation was employed in all cases<sup>[15]</sup> along with the local exchange–correlation potential of Vosko, Wilk, and Nusair<sup>[16]</sup> and

gradient corrections to exchange (Becke)<sup>[17]</sup> and correlation (Perdew).<sup>[18]</sup> Unsubstituted Cp rings, constrained to local *D*<sub>5h</sub> symmetry, were used to model Cp\* ligands. The broken-symmetry methodology,<sup>[19]</sup> which involves the removal of all symmetry elements connecting the ruthenium centers (corresponding to a reduction in symmetry from *C*<sub>2h</sub> to *C*<sub>s</sub>), was used for all singlet configurations.

Received: February 18, 2000 [Z14736]

- [1] W.-D. Stohrer, R. Hoffmann, *J. Am. Chem. Soc.* **1972**, *94*, 1661–1668.
- [2] J. Chatt, L. Manojlovic-Muir, K. W. Muir, *J. Chem. Soc. Chem. Commun.* **1971**, 655–656.
- [3] K. Wieghardt, G. Backes-Dahmann, B. Nuber, J. Weiss, *Angew. Chem.* **1985**, *97*, 773–774; *Angew. Chem. Int. Ed. Engl.* **1985**, *24*, 777–778.
- [4] A. Bashall, V. C. Gibson, T. P. Kee, M. McPartlin, O. B. Robinson, A. Shaw, *Angew. Chem.* **1991**, *103*, 1021–1023; *Angew. Chem. Int. Ed. Engl.* **1991**, *30*, 980–982.
- [5] Y. Jean, A. Lledos, J. K. Burdett, R. Hoffmann, *J. Am. Chem. Soc.* **1988**, *110*, 4506–4516.
- [6] J. Song, M. B. Hall, *Inorg. Chem.* **1991**, *30*, 4433–4437.
- [7] a) K. Yoon, G. Parkin, A. L. Rheingold, *J. Am. Chem. Soc.* **1991**, *113*, 1437–1438; b) K. Yoon, G. Parkin, A. L. Rheingold, *J. Am. Chem. Soc.* **1992**, *114*, 2210–2218.
- [8] G. Parkin, *Chem. Rev.* **1993**, *93*, 887–909.
- [9] a) U. Kölle, J. Kossakowski, N. Klaff, L. Wesemann, U. Englert, G. E. Heberich, *Angew. Chem.* **1991**, *103*, 732–733; *Angew. Chem. Int. Ed. Engl.* **1991**, *30*, 690–691; b) U. Kölle, H. Lueken, K. Handrick, K. Schilder, J. K. Burdett, S. Balleza, *Inorg. Chem.* **1995**, *34*, 6273–6278.
- [10] G. Parkin, R. Hoffmann, *Angew. Chem.* **1994**, *106*, 1530; *Angew. Chem. Int. Ed. Engl.* **1994**, *33*, 1462.
- [11] P. Gutlich, H. A. Goodwin, D. N. Hendrickson, *Angew. Chem.* **1994**, *106*, 441–443; *Angew. Chem. Int. Ed. Engl.* **1994**, *33*, 425–426.
- [12] a) J. E. McGrady, T. Lovell, R. Stranger, *Inorg. Chem.* **1997**, *36*, 3242–3247; b) J. E. McGrady, R. Stranger, T. Lovell, *J. Phys. Chem. A* **1997**, *101*, 6265–6272.
- [13] R. Poli, H. D. Mui, *Inorg. Chem.* **1991**, *30*, 65–77.
- [14] a) ADF 99, E. J. Baerends, A. Bérces, C. Bo, P. M. Boerrigter, L. Cavallo, L. Deng, R. M. Dickson, D. E. Ellis, L. Fan, T. H. Fischer, C. Fonseca Guerra, S. J. A. van Gisbergen, J. A. Groeneveld, O. V. Gritsenko, F. E. Harris, P. van den Hoek, H. Jacobsen, G. van Kessel, F. Kootstra, E. van Lenthe, V. P. Osinga, P. H. T. Philipsen, D. Post, C. C. Pye, W. Ravenek, P. Ros, P. R. T. Schipper, G. Schreckenbach, J. G. Snijders, M. Sola, D. Swerhone, G. te Velde, P. Vernooijs, L. Versluis, O. Visser, E. van Wezenbeek, G. Wiesenekker, S. K. Wolff, T. K. Woo, T. Ziegler, Scientific Computing and Modelling NV, Amsterdam, Netherlands; b) C. Fonseca Guerra, J. G. Snijders, G. te Velde, E. J. Baerends, *Theor. Chem. Acc.* **1998**, *99*, 391–403.
- [15] R. G. Parr, W. Yang, *Density Functional Theory of Atoms and Molecules*, Oxford University Press, New York, **1989**.
- [16] S. H. Vosko, L. Wilk, M. Nusair, *Can. J. Phys.* **1980**, *58*, 1200–1211.
- [17] A. D. Becke, *Phys. Rev. A* **1988**, *38*, 3098–3100.
- [18] J. P. Perdew, *Phys. Rev. B* **1986**, *33*, 8822–8824.
- [19] L. Noodleman, D. A. Case, *Adv. Inorg. Chem.* **1992**, *38*, 423–470.